

## Algorithm of Management of Patients With Parotid Gland Tumors

*Latipova D. I.*

*Independent researcher of the Department of Maxillofacial Surgery  
Tashkent State Medical University*

**Abstract:** Neoplasms of the salivary glands are benign in most cases and in up to 80% of cases are localized in the parotid salivary gland (PSG). The features of the PSG structure, as well as the anatomical area in which the gland is located, and adjacent structures largely determine the high requirements for a set of diagnostic measures and surgical treatment tactics. The article is devoted to the analysis of the effectiveness of the proposed scheme of diagnostic and therapeutic measures for PSG neoplasms, which includes the results of radiomic analysis of MRI and CBCT, ultrasound of the area of interest with the identification of characteristic signs of nosological forms.

**Keywords:** neoplasms of the salivary glands, parotid salivary gland, diagnosis, epidemiology, multispiral computed tomography, magnetic resonance imaging, pathohistological examination, radiomic analysis.

**Introduction.** As is known, neoplasms of the salivary glands are among the most difficult in maxillofacial surgery for diagnosis and treatment. According to statistics, among all salivary glands, tumors of the parotid gland account for 92%, the submandibular gland – 6.5%, the sublingual gland – 0.5%, and the small salivary glands – 1%. Bradley A. Schiff (2022) noted that the risk of malignancy is higher with small salivary glands (for example, the parotid gland has a lower risk of malignancy than small salivary glands) [1, 3].

About 85% of salivary gland tumors affect the PSG, less often the submandibular and small salivary glands, and about 1% of tumors occur in the sublingual glands. About 75-80% of tumors are benign, slow-growing, mobile, painless, and dense nodules are usually detected under the skin or mucosa [2, 4, 5].

For the purpose of preliminary diagnosis, in order to determine the adequate scope of future surgical treatment, any surgical intervention on the parotid salivary glands is preceded by a clinical, laboratory and special examination. And an accurate diagnosis is made only on the basis of cytomorphological examination of the tissues of the removed neoplasm.

According to Kuzmina E.V. (2023), the frequency of diagnostic errors in patients with neoplasms of the salivary glands remains high. Clinical examination of patients with this pathology should be complemented by the results of cytological examination, since none of the methods makes it possible to accurately diagnose [2, 6].

However, it should be borne in mind that fine needle aspiration cytological examination (FNAC) is invasive, and due to the heterogeneity of the neoplasm, the accuracy in its characterization is only 86-95%, while 5-14% of the results remain unknown, which leads to the need for re-diagnosis. Only a comprehensive analysis makes it possible to reduce the number of diagnostic errors and, subsequently, errors in choosing surgical treatment tactics [7-10, 16].

Recently, a new area of in-depth digital image analysis has been actively developing – radiomics, the concept of which was proposed in 2012 and includes high-performance extraction, analysis and interpretation of quantitative features from medical images. Textural image analysis is a part of radiomics and provides an objective quantitative assessment of tumor heterogeneity by distributing and correlating pixel levels or gray voxels in an image [11-15, 17].

Given the non-invasiveness of the radiomic method, textural image analysis can be presented as a "virtual biopsy". The purpose of radiomics and textural analysis is to build a standardized predictive model for determining clinical outcomes with selected features. The main diagnostic task of radiomics in oncology is to accurately distinguish between benign and malignant tumors using non-invasive diagnostic methods.

Based on this, the above issues of developing an algorithm for the comprehensive diagnosis of salivary gland neoplasms are currently relevant and directly affect the success of treatment.

**The aim of the study** is to develop a strategy for diagnostic and therapeutic measures for PSG neoplasms and to substantiate its clinical effectiveness.

**Materials and Methods.** To achieve this goal, we analyzed the data of 124 patients with PSG neoplasms who received inpatient treatment at the Department of Adult Maxillofacial Surgery at the Tashkent State Dental Institute Clinic in the period 2022-2024 in order to identify specific signs, which were further compared with the results of a pathomorphological study. The neoplasms were divided into nosological forms according to the international histological classification of salivary gland tumors (WHO, 2022).

The LIFEx program (versions for ultrasound, CT, and MRI image analysis) is used for textural image analysis. The choice of this program was due to its free access, intuitive and simple user interface for operation, regular improvement of the program by developers and the release of updates with new functionality and the elimination of minor flaws, as well as the lack of requirements for powerful computer computing abilities. LIFEx participates in the Biomarker Imaging Standardization Initiative (BISI).

The protocol for the textural analysis of ultrasound, CT, and MRI images included five sequential actions: pre-processing, segmentation of the neoplasm (delineation of areas of interest or ROI), extraction of textural features, feature selection, and development of a predictive classification model. In total, data from 38 ultrasound examinations, 62 MSCT and 97 MRI were processed.

Further, after training the model, the program was applied to 28 patients with PSG neoplasms who applied to the clinic of the adult Clinical Hospital of the Tashkent State Medical University Dental Clinic, and 25 patients who were treated at the Department of Clinical Hospital of the Republican Specialized Scientific and Practical Medical Center for Otorhinolaryngology and Head and Neck Diseases (RSPMC of Otorhinolaryngology and Head and Neck Diseases). The results were compared with the conclusions of a pathohistological study performed at the center and various private laboratories. Based on the effectiveness of the program and the specificity of the signs of each type of neoplasm, the following algorithm of therapeutic and diagnostic measures for PSG tumors was compiled.

The data was analyzed using descriptive statistics. Statistical processing of the obtained data was carried out using nonparametric methods (Mann-Whitney criterion) and correlation analysis (Pearson criterion). The results were presented as a median, and the reliability of the difference in average values was evaluated according to the Student's criterion. The principles of evidence-based medicine are used in the organization and conduct of research. The statistical analysis was performed using the OriginPro 8.6 program (OriginLab Corporation, USA).

**Results and Discussion.** Initially, PSG neoplasms were assessed on slices based on the following criteria: localization, size, shape, contour clarity, homogeneity/inhomogeneity of structure, average density, presence or absence of signs of invasive growth in adjacent anatomical structures, the presence of lymphadenopathy of regional lymph nodes and invasion of facial nerve trunks.

Based on the results of the ultrasound study, the characteristic signs for each type of PSG neoplasm registered in the medical documentation for the period under study were identified. The structural features were also studied by color Doppler mapping (CDM).

According to the results of CT and MRI analysis, the sizes of benign and malignant PSG tumors varied widely, and according to statistics, the average size of malignant tumors was significantly larger than benign ones,  $35.5 \pm 5.9$  and  $18.4 \pm 3.7$  mm, respectively. However, this feature is impractical for differential diagnosis due to its very low specificity. The shape and contours of the neoplasms turned out to be more significant signs. In benign tumors, the shape of the formation in the images is usually regular, rounded, oval or lobed, and the contours are clear and can be traced along the entire perimeter of the neoplasm. And with malignant tumors, irregular shape and indistinctness of contours along most of the perimeter with the presence of invasive growth.

The differential diagnostic and prognostic value of diffusion-weighted MRI with the construction of maps of the measured diffusion coefficient (ADC) and the automatic determination of ADC coefficients was studied. At the same time, the optimal value of the cut-off threshold was previously determined as  $1.1 \times 10^{-3}$  mm/sec, that is, ADC values below  $1.1 \times 10^{-3}$  mm/sec indicated the probability of a malignant lesion, above  $1.1 \times 10^{-3}$  mm/sec – benign.

The characteristic values for the types of benign PSG lesions were also determined:

pleomorphic adenoma –  $(1,76 \pm 0,15) \times 10^{-3}$  mm/sec,

adenolymphoma –  $(0,79 \pm 0,04) \times 10^{-3}$  mm/sec,

lymphangioma –  $(0,58 \pm 0,03) \times 10^{-3}$  mm/sec,

benign neoplasm –  $(1,35 \pm 0,24) \times 10^{-3}$  mm/sec,

malign neoplasm –  $(0,98 \pm 0,05) \times 10^{-3}$  mm/sec.

Using computer-assisted processing, programmers extracted 38 textural indicators characterizing intra-tumor spatial heterogeneity: 6 from the histogram of signal distribution (DISCRETIZED\_HISTO), 6 from the matrix of gray level coincidence (GLCM–gray level coocurrence matrix), 1 from the matrix of gray level length segments (GLRLM-gray level run length matrix), 3 – from the differentiated matrix of neighboring gray levels (NGLDM Neiborhood gray-level difference matrix) and 1 – from the matrix of zone lengths of gray levels (GLZLM-gray level zone length matrix). Next, the five most significant textural features were selected. In addition to identifying the characteristic features of the images, a comparative analysis was performed with the average values of the ADC and ULTRASOUND signs to increase the sensitivity (88.2%) and specificity (90.7%) of the diagnosis.

In accordance with the results of the analysis of the significance of ultrasound, CBCT and MRI signs, and a critical analysis of the effectiveness of various types of surgical interventions, a therapeutic and diagnostic algorithm was developed (Fig. 1).

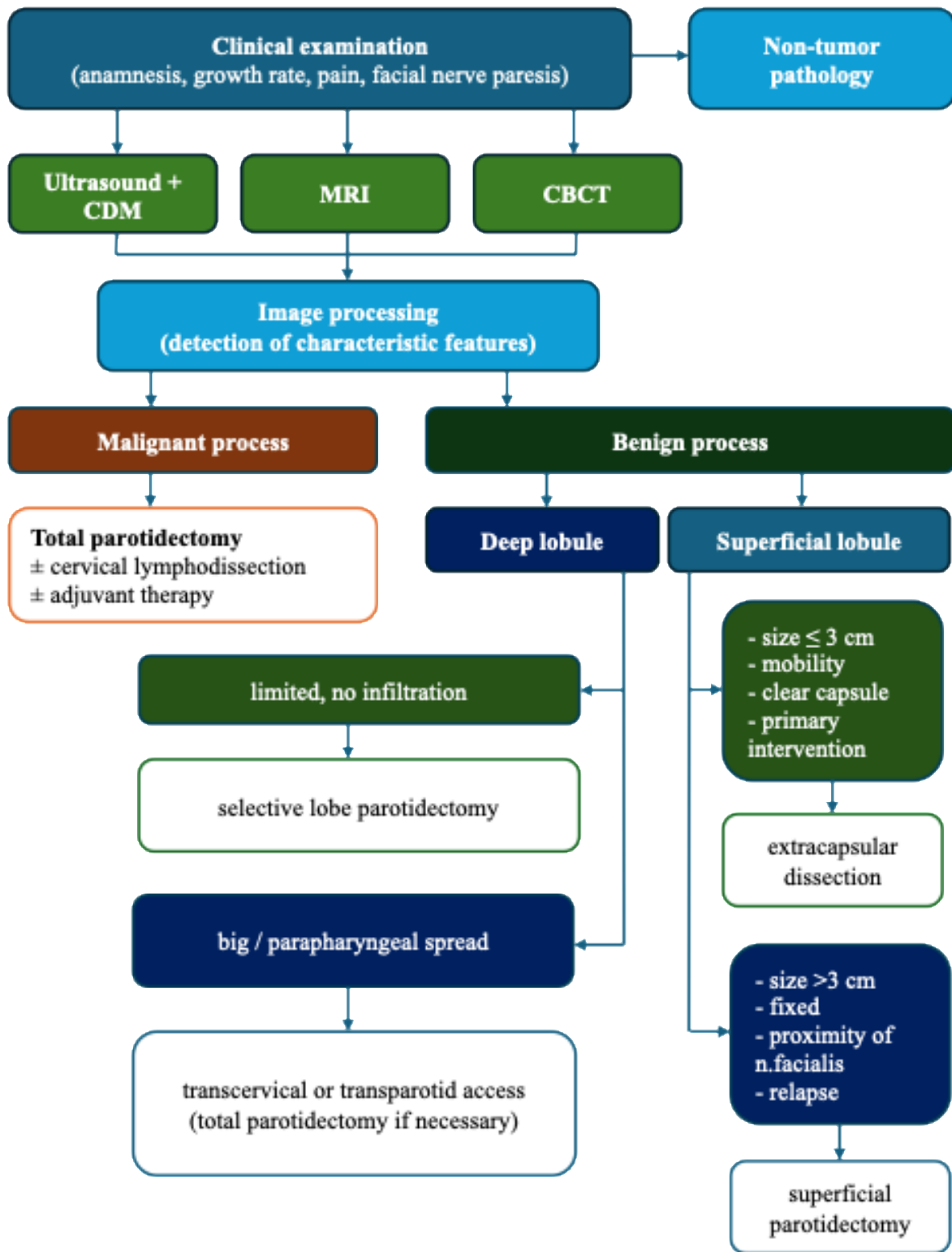


**Fig. 1. Therapeutic and diagnostic algorithm for PSG tumors**

**Clinical case.** Patient N.D., 38 years old, complaining of a painless swelling in the right parotid-masticatory region. The skin above the swelling is unchanged, it gathers into a fold. On palpation, the formation is mobile, dense, and the surface is bumpy. Ultrasound of the right PSG revealed the formation of reduced echogenicity, with a moderately heterogeneous echostructure and uneven but clear contours. The capsule is well visualized (Fig. 2). Single vascular structures of small diameter with low-velocity blood flow along the periphery were found in the CDM mode (Fig. 3).

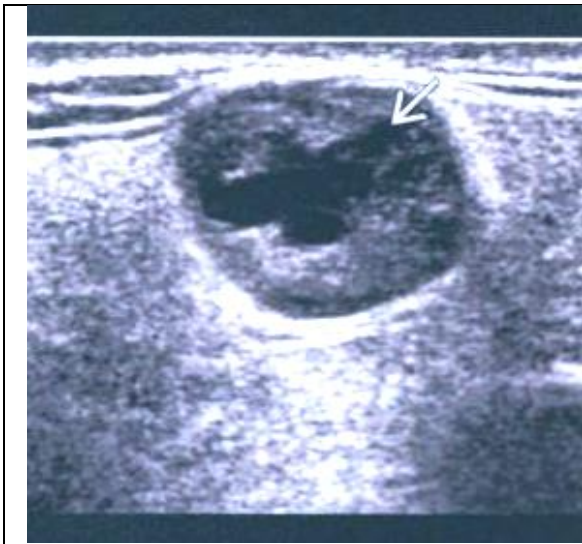


Fig. 2. Ultrasound visualization of a pleomorphic adenoma of the right cerebrospinal fluid, formation with a moderately heterogeneous echo structure and uneven but clear contours;

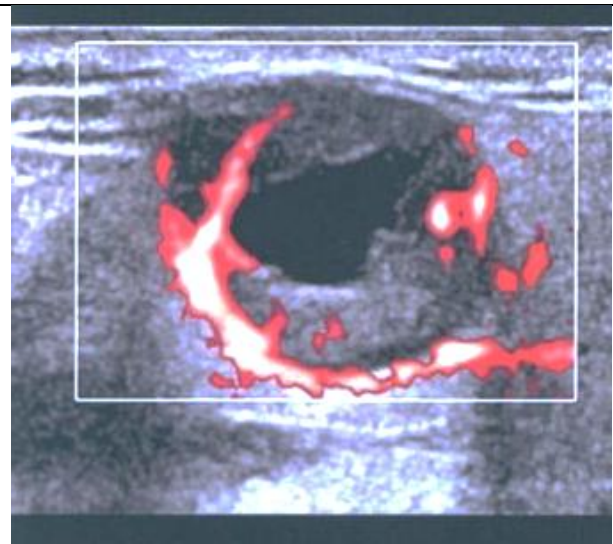
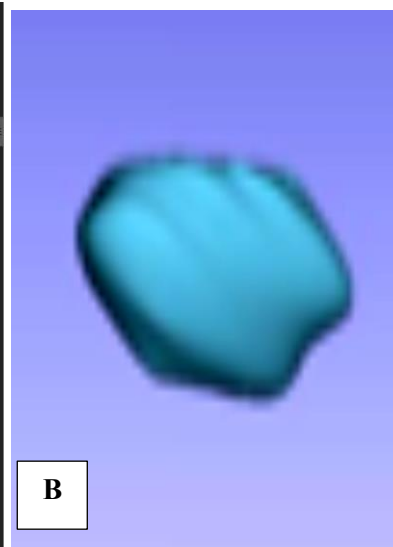
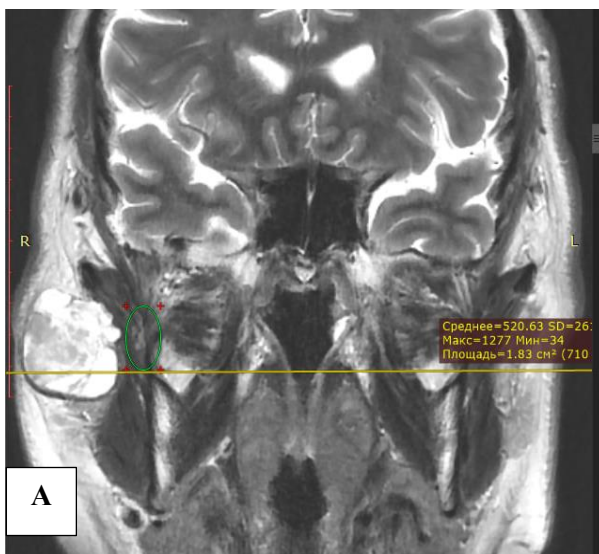
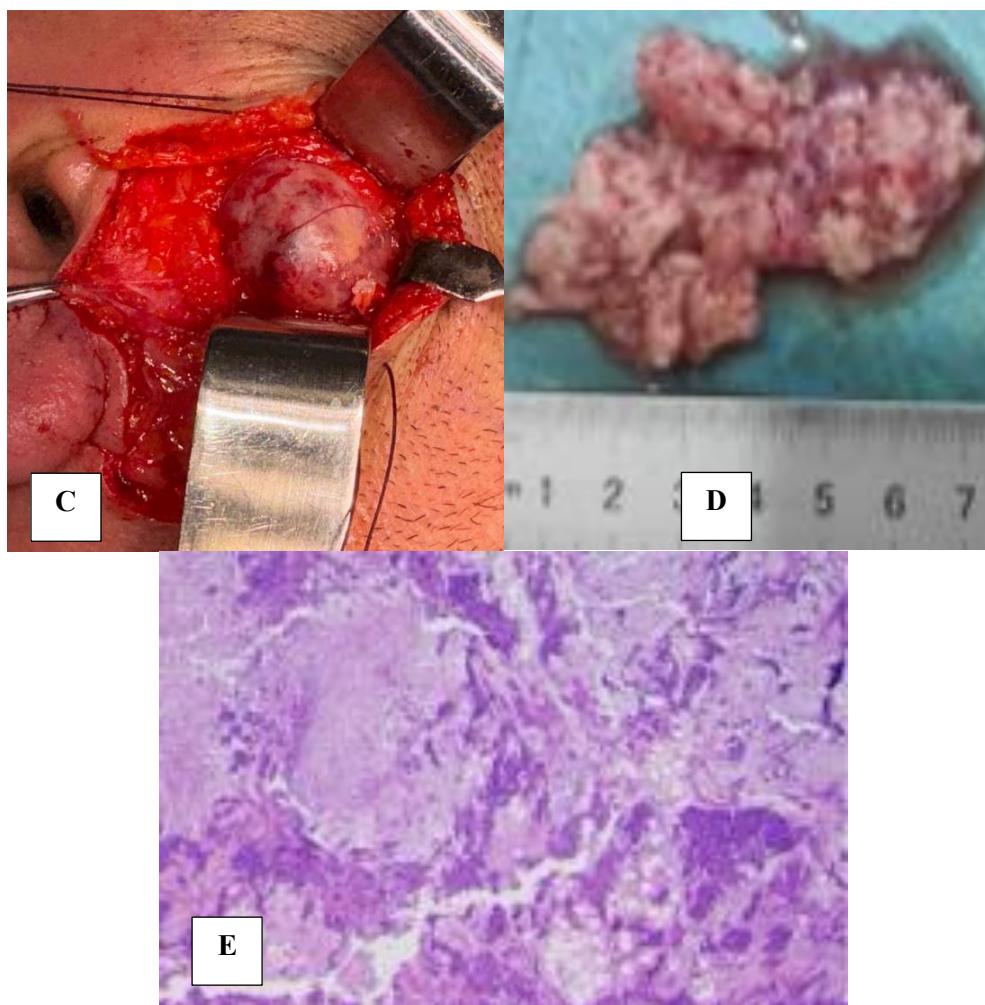


Fig. 3. Ultrasound visualization of a pleomorphic adenoma of the right cerebrospinal fluid, single vascular structures of small diameter in the CDM regime

An oval-shaped, lobular structure with clear contours was found on the MRI slices in the superficial lobe of the PSG. The capsule can be traced along the entire perimeter of the neoplasm. The ADC value is  $1.62 \times 10^{-3}$  mm<sup>2</sup>/sec. Segmentation and digital processing of T2-weighted MRI images of the area of interest from various projections were performed, as well as 3D reconstruction of the neoplasm using 3D Slicer software (Fig. 4). Textural analysis of the images revealed a benign neoplasm (5x4 cm) in the projection of the superficial lobe of the PSG. The neoplasm was removed along with the capsule (formation in the section of white color, soft consistency). Pathohistological examination confirmed the primary clinical diagnosis – pleomorphic adenoma of the PSG.





**Fig. 4. Clinical example: A – MRI imaging in coronal and axial projections; B – 3D reconstruction of the area of interest; C – photo from the surgery; D – macro preparation of the neoplasm; E – micro preparation (Romanovsky-Giemsa staining, x100)**

**Conclusions.** Thus, textural analysis of ultrasound, CBCT and MRI data is an important component in the diagnosis of parotid salivary gland neoplasms, which provides valuable additional quantitative information about the structural features of tissues and reveals the most specific signs of each nosological form. The radiomic analysis program requires further improvement to increase sensitivity and specificity. The developed therapeutic and diagnostic algorithm for the management of patients with PSG neoplasms has demonstrated high efficiency and accuracy by significantly reducing the risk of diagnostic errors, subsequently leading to the choice of the wrong method of surgical treatment, relapses and repeated interventions.

#### References

1. Iordanishvili A.K., Lobeyko V.V. Prevalence of salivary gland diseases in adults at different age periods // *Clinical gerontology*. 2014. – №20 (11-12). – Pp. 14-19.
2. Kuzmina E.V., Sotnikova M.V., Borovoy V.N., Nakonechny D.A. Problems of diagnosis of neoplasms of salivary glands. – *Clinical dentistry*. – 2023; 26 (3): 60-69.
3. Tarakanova O.V., Slavnova E.N. Cytological diagnosis of salivary gland tumors. *Oncology*. P.A. Herzen Magazine. 2022;11(5):78 88.
4. Shomurodov K.E., Latipova D.I., Alimdzhanova M.S. The prevalence of parotid salivary gland neoplasms and key aspects of their diagnosis. *Integrative dentistry and maxillofacial surgery*. 2024;3(3):65-71.

5. Shumkova E.N., Balapanova A.Kh., Alsherieva U.A., Iskakov A.J. Clinical and morphological aspects of salivary gland tumors. — Bulletin of Science and Education. — 2020; 14—1 (92): 74-76.
6. Abbate, V.; Orabona, G.D.A.; Barone, S.; Troise, S.; Bonavolontà, P.; Pacella, D.; Iaconetta, G.; Califano, L. Relevance of Inflammatory Biomarkers in Salivary Gland Cancers Management. *Eurasian J. Med. Oncol.* 2021, 5, 311-317.
7. Alsanie I, Rajab S, Cottom H, et al. Distribution and Frequency of Salivary Gland Tumours: An International Multicenter Study. *Head Neck Pathol.* 2022;16(4):1043-1054.
8. Atamaniuk V, Chen J, Obrzut M, et al. High-frequency shear wave MR elastography of parotid glands: custom driver design and preliminary results. *Sci Rep.* 2024;14(1):24496. Published 2024 Oct 18.
9. Cheng, G.; Liu, F.; Niu, X.; Fang, Q. Role of the pretreatment neutrophil-to-lymphocyte ratio in the survival of primary parotid cancer patients. *Cancer Manag. Res.* 2019, 11, 2281–2286.
10. Damar, M.; Dinç, A.E.; Erdem, D.; Aydil, U.; Kizil, Y.; Eravcı, F.C.; Bişkin, S.; Şevik Eliçora, S.; Işık, H. Pretreatment Neutrophil-Lymphocyte Ratio in Salivary Gland Tumors Is Associated with Malignancy. *Otolaryngol. Head Neck Surg.* 2016, 155, 988-996.
11. Ghaderi, Hamid, Kruger, Estie, Ahmadvand, Simin, Mohammadi, Yousef, Khademi, Bijan, Ghaderi, Abbas, Epidemiological Profile of Salivary Gland Tumors in Southern Iranian Population: A Retrospective Study of 405 Cases, *Journal of Cancer Epidemiology*, 2023, 8844535, 11 pages, 2023.
12. Nardone, V.; Reginelli, A.; Grassi, R.; Boldrini, L.; Vacca, G.; D'Ippolito, E.; Annunziata, S.; Farchione, A.; Belfiore, M.P.; Desideri, I.; et al. Delta radiomics: A systematic review. *Radiol. Med.* 2021, 126, 1571–1583.
13. Peravali RK, Bhat HH, Upadya VH, Agarwal A, Naag S. Salivary gland tumors: a diagnostic dilemma!. *J Maxillofac Oral Surg.* 2015;14(Suppl 1):438-442.
14. Rossi ED, Faquin WC, Baloch Z, Barkan GA, Foschini MP, Pusztaszeri M, Vielh P, Kurtycz DFI. The Milan System for Reporting Salivary Gland Cytopathology: analysis and suggestions of initial survey. *Cancer Cytopathol.* 2017;125(10):757-766.